Publications   Educational Psychology and Special Education

2012

Power Method Distributions through Conventional Moments and L-Moments

Flaviu A. Hodis
Victoria University of Wellington

Todd C. Headrick
Southern Illinois University Carbondale, headrick@siu.edu

Yanyan Sheng
Southern Illinois University Carbondale

Power Method Distributions
through Conventional Moments and *L*-Moments

Flaviu A. Hodis

Victoria University of Wellington
P.O. Box 17-310, Karori, Wellington, New Zealand
flaviu.hodis@vuw.ac.nz

Todd C. Headrick[*] **and Yanyan Sheng**

Section on Statistics and Measurement, Department EPSE, 222-J Wham Bldg.
Southern Illinois University Carbondale, Carbondale, IL USA 62901-4618
headrick@siu.edu

Abstract

This paper develops two families of power method (PM) distributions based on polynomial transformations of the (1) Uniform, (2) Triangular, (3) Normal, (4) D-Logistic, and (5) Logistic distributions. One family is developed in the context of conventional method of moments and the other family is derived through the method of *L*-moments. As such, each of the five conventional moment-based PM classes has an analogous *L*-moment based class. A primary focus of the development is on PM polynomial transformations of order three. Specifically, systems of equations are derived for computing polynomial coefficients for user specified values of skew (*L*-skew) and kurtosis (*L*-kurtosis). Boundary regions for determining feasible combinations of skew (*L*-skew) and kurtosis (*L*-kurtosis) are also derived for determining if a set of solved coefficients yields a valid PM probability density function. Further, the conventional moment-based family of PM distributions is compared with its *L*-moment based analog in terms of estimation, power, outliers, and distribution fitting. The results of the comparison demonstrate that the *L*-moment based PM family is superior to the conventional moment-based family in each of the categories considered.

Mathematics Subject Classification: 65C05, 65C10, 65C60

Keywords: Monte Carlo, Power Method, Simulation, Skew, Kurtosis, *L*-skew, *L*-kurtosis

---

[*]Corresponding author

1 Introduction

The power method (PM) polynomial transformation is a traditional moment-matching procedure used for simulating univariate and multivariate non-normal distributions (see [1]-[4]). The power method has been used in studies that have included such topics or techniques as: ANCOVA [5]-[6], asset pricing theories [7], item response theory [8], microarray analysis [9], multivariate analysis [10], nonparametric statistics [11], price risk [12], regression [13], structural equation models [14], and toxicology research [15]. The PM is also useful for simulating correlated non-normal distributions with specific types of structures. Some examples include continuous non-normal distributions correlated with ranked variables, systems of linear statistical models, and distributions with specified intraclass correlations (see [4]).

The basic univariate third-order PM transformation originally proposed by Fleishman [1] proceeds by taking the sum of a linear combination of a standard normal random variable (Z), its square, and its cube as

$$p(Z) = c_1 + c_2 Z + c_3 Z^2 + c_4 Z^3. \tag{1}$$

The coefficients (c_i) in (1) can be determined by simultaneously solving Headrick's Equations (2.18)–(2.21) ([4], p.15) for specified values of conventional skew (γ_3) and kurtosis (γ_4). On solving these equations the values of c_i are substituted into (1) to produce $p(Z)$, which has zero mean, unit variance, and the desired values of γ_3 and γ_4.

Although the traditional PM is often used, it has the limitations associated with conventional moments insofar as estimates of γ_3 and γ_4 that can be substantially biased, have high variance, or can be influenced by outliers (e.g. [16], p.4). However, some of these limitations were addressed by Headrick [16] where the standard normal-based PM in (1) was derived in the context of L-moment theory [17]. The primary advantage of the L-moment based PM transformation is that estimates of L-skew (τ_3) and L-kurtosis (τ_4) are nearly unbiased for any sample size and have smaller variance than their conventional moment based counterparts of γ_3 and γ_4.

Another limitation associated with the third-order PM in (1) is that it does not span the entire region of all possible combinations of γ_3 and γ_4 defined in the plane as (e.g. [4], p.26)

$$\gamma_4 \geq \gamma_3^2 - 2, \tag{2}$$

where the normal distribution is scaled such that $\gamma_4 = 0$. For example, the polynomial transformation in (1) will not produce PM distributions with valid probability density functions for $\gamma_4 < 0$ ([4], p.21).

In view of the above, one of the primary goals of this paper is to develop a conventional moment-based family of PM distributions that expands the PM's coverage in γ_3 and γ_4 plane defined by (2). More specifically, in the context

of symmetric third-order polynomials, the kurtosis boundary will be extended from $0 < \gamma_4 < 43.2$, which is associated with (1), to $-1.2 < \gamma_4 < 472.5$, which is based on five distributions: (1) Uniform, (2) Triangular, (3) Normal, (4) D-Logistic, and (5) Logistic. Further, another goal of this paper is to obviate the limitations associated with estimates of γ_3 and γ_4 in the contexts of bias and efficiency by deriving the *L*-moment based family of PM distributions that is analogous to the proposed conventional moment based family. In so doing, the *L*-moment based family of PM distributions has distinct advantages over the conventional PM family in these contexts. In particular, these advantages become more substantial when distributions with more extreme departures from normality (e.g. distributions with heavy tails) are considered.

The remainder of this paper is outlined as follows. In Section 2, the essential requisite information and general notation are provided for both conventional and *L*-moment based PM polynomials. The five conventional and *L*-moment based systems of equations for computing polynomial coefficients for each class considered are subsequently developed as well as the derivation of the boundary conditions to determine if any particular PM transformation has an associated valid pdf. In Section 3, the conventional moment and *L*-moment based families are compared in terms of estimation, power, outliers, and distribution fitting to demonstrate the superior characteristics that *L*-moments have in these contexts.

2   Methodology

2.1   Preliminaries

Let W be a continuous random variable with zero mean, unit variance, probability density function (pdf), and cumulative distribution function (cdf) defined as

$$f_W(w) = \phi_j(w) \tag{3}$$
$$F_W(w) = \Phi_j(w) \tag{4}$$

where the pdf $\phi_j(w)$ is symmetric ($\gamma_3 = 0$) and has specific forms of: $\phi_1(w) \equiv$ Uniform, $\gamma_4 = -1.2$; $\phi_2(w) \equiv$ Triangular, $\gamma_4 = -0.6$; $\gamma_3(w) \equiv$ Normal, $\gamma_4 = 0.0$; $\phi_4(w) \equiv$ D-Logistic, $\gamma_4 = +0.6$; and $\phi_5(w) \equiv$ Logistic, $\gamma_4 = +1.2$. The functional forms, graphs, moments, and Gini's indices associated with these five pdfs are given in Figure 1 and Table 1. Note that the D-Logistic (Triangular) distribution can be defined as the sum of two independent Logistic

(Uniform) random variables. The specific forms of the cdf in (4) are

$$\Phi_1(w) = (w + \sqrt{3}) \big/ (2\sqrt{3}), -\sqrt{3} < w < +\sqrt{3} \tag{5}$$

$$\Phi_2(w) = \begin{cases} (w + \sqrt{6})^2 /12 \\ (\sqrt{6} - w)^2 /12 \end{cases}, -\sqrt{6} < w < +\sqrt{6} \tag{6}$$

$$\Phi_3(w) = \frac{1}{\sqrt{2\pi}} \int_{-\infty}^{w} \exp\{\frac{-u^2}{2}\}du, -\infty < w < +\infty \tag{7}$$

$$\Phi_4(w) = 1 - \frac{(\exp\{-dw\}(\exp\{-dw\} - 1 + dw))}{(1 - \exp\{-dw\})^2}, -\infty < w < +\infty \tag{8}$$

$$\Phi_5(w) = 1 \big/ ((1 + \exp\{-(\pi/\sqrt{3})w\})), -\infty < w < +\infty \tag{9}$$

where $d = \sqrt{2}\pi \big/ \sqrt{3}$ in (8).

Distribution	μ_4	μ_6	μ_8	μ_{10}	μ_{12}	$\Delta/2$
Uniform	$\dfrac{9}{5}$	$\dfrac{27}{7}$	$\dfrac{45}{5}$	$\dfrac{243}{11}$	$\dfrac{25515}{455}$	$\dfrac{1}{\sqrt{3}}$
Triangular	$\dfrac{12}{5}$	$\dfrac{54}{7}$	$\dfrac{144}{5}$	$\dfrac{1296}{11}$	$\dfrac{233280}{455}$	$\dfrac{7}{5\sqrt{6}}$
Normal	$\dfrac{15}{5}$	$\dfrac{105}{7}$	$\dfrac{525}{5}$	$\dfrac{10395}{11}$	$\dfrac{4729725}{455}$	$\dfrac{1}{\sqrt{\pi}}$
D-Logistic	$\dfrac{18}{5}$	$\dfrac{180}{7}$	$\dfrac{1512}{5}$	$\dfrac{58320}{11}$	$\dfrac{59105376}{455}$	$\dfrac{3 + \pi^2}{3\pi\sqrt{6}}$
Logistic	$\dfrac{21}{5}$	$\dfrac{279}{7}$	$\dfrac{3429}{5}$	$\dfrac{206955}{11}$	$\dfrac{343717911}{455}$	$\dfrac{\sqrt{3}}{\pi}$

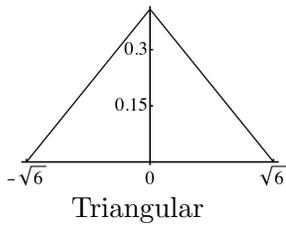Table 1: The relevant moments and Gini's indices (Δ) associated with the pdfs in Figure 1

Given (3) and (4), the power method (PM) polynomial in (1) can be more generally expressed as

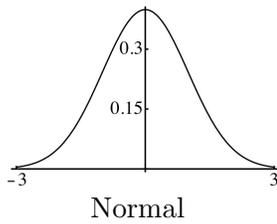$$p(W) = \sum_{i=1}^{m} c_i W^{i-1} \tag{10}$$

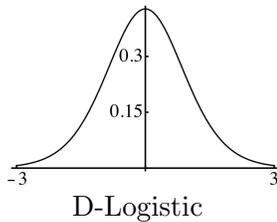where setting $m = 4$ yields a third-order polynomial.

$$\phi_1(w) = 1\left/\left(2\sqrt{3}\right)\right., -\sqrt{3} < w < +\sqrt{3}$$

Uniform
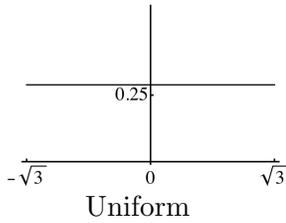
$$\phi_2(w) = \begin{cases} (1/6)(w + \sqrt{6}), -\sqrt{6} < w < 0 \\ (1/6)(\sqrt{6} - w), 0 < w < \sqrt{6} \end{cases}$$
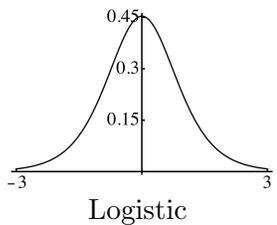
Triangular

$$\phi_3(w) = (2\pi)^{-\frac{1}{2}}\exp\{-w^2/2\}, -\infty < w < +\infty$$

Normal

$$\phi_4(w) = \frac{d(\exp\{dw\}(2 + \exp\{dw\}(dw - 2) + dw))}{(\exp\{dw\} - 1)^3}, -\infty < w < +\infty$$

$$d = \sqrt{2}\pi\left/\sqrt{3}\right.$$

D-Logistic

$$\phi_5(w) = \frac{(\pi\left/\sqrt{3}\right.)(\exp\{-w(\pi\left/\sqrt{3}\right.)\})}{(1 + \exp\{-w(\pi\left/\sqrt{3}\right.)\})^2}, -\infty < w < +\infty$$

Logistic

Figure 1: Probability density functions associated with the Power Method families of distributions.

The pdf and cdf associated with $p(W)$ in (10) are given as in [4] (see p.12)

$$f_{p(W)}(p(w)) = \bar{f}(w) = \left(p(w), \frac{f_W(w)}{p'(w)}\right) \tag{11}$$

$$F_{p(W)}(p(w)) = \bar{F}(z) = (p(w), F_W(w)) \tag{12}$$

where $\bar{f} : \mathbb{R} \to \mathbb{R}^2$ and $\bar{F} : \mathbb{R} \to \mathbb{R}^2$ are the parametric forms of the pdf and cdf with the mappings $z \to (x, y)$ and $z \to (x, v)$ with $x = p(w)$, $y = (f_W(w))/p'(w)$, and $v = F_W(w)$, respectively. It is assumed that $p'(w) > 0$ in (11), that is, the transformation in (10) must be a strictly increasing monotone function for a valid PM pdf to exist. Note also that the PM pdf and cdf in (11) and (12) have the forms of (3) and (4) for the special case of when $c_2 = 1$ and $c_{i \neq 2} = 0$ in (10).

2.2 The conventional moment third-order power method family

Given the preliminaries from the previous section, the first task is to determine the systems of equations for computing the coefficients (c_i) associated with polynomials of the form in (10) with $m = 4$ for each of the five PM classes. This can be accomplished by making use of the general equations for the mean (γ_1), variance (γ_2), skew (γ_3), and kurtosis (γ_4) for any third-order PM distribution given in [4] (see p.15) as

$$\gamma_1 = 0 = c_1 + c_3 \tag{13}$$
$$\gamma_2 = 1 = c_2^2 + (\mu_4 - 1)c_3^2 + \mu_4 2c_2 c_4 + \mu_6 c_4^2 \tag{14}$$
$$\gamma_3 = (\mu_4 - 1)c_2^2 c_3 + (\mu_6 - 3\mu_4 + 2)c_3^3 + (\mu_6 - \mu_4)6c_2 c_3 c_4 + \\ (\mu_8 - \mu_6)3c_3 c_4^2 \tag{15}$$
$$\gamma_4 = -3 + \mu_1 2c_4^4 + \mu_4 c_2^4 + \mu_6 4c_2^3 c_4 + (\mu_{10} - 2\mu_8 + \mu_6)6c_3^2 c_4^2 \\ + (\mu_8 - 4\mu_6 + 6\mu_4 - 3)c_3^4 + 6c_2^2((\mu_6 - 2\mu_4 + 1)c_3^2 + \mu_8 c_4^2) \\ + 4c_2 c_4(\mu_{10}c_4^2 + (\mu_8 - 2\mu_6 + \mu_4)3c_3^2). \tag{16}$$

Substituting the even moments for the five pdfs $\phi_j(w)$ given in Table 1 yields the specific forms of (13)–(16), which are given in Figure 2 through Figure 6. Each of the five systems of equations in these figures consists of four equations where the first two equations for the mean and variance are set to zero and one, respectively. The last two equations of the form in (15) and (16) are set to specified values of skew and kurtosis. Simultaneously solving any particular set of four equations will yield the coefficients for polynomials of the form in (10).

In general, if the coefficients with odd subscripts in (10) are zero (i.e. $c_1 = c_3 = 0$), then any PM distribution is symmetric. Further, when solving for
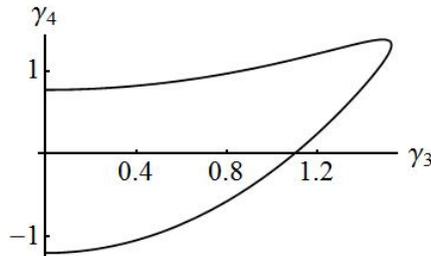
(1) Conventional Moment PM Uniform System:

$$\gamma_1 = 0 = c_1 + c_3$$

$$\gamma_2 = 1 = c_2^2 + 4c_3^2/5 + 18c_2c_4/5 + 27c_4^2/7$$

$$\gamma_3 = 4(75075c_2^2c_3 + 14300c_3^3 + 386100c_2c_3c_4 + 482625c_3c_4^2)/125125$$

$$\gamma_4 = 9c_2^4/5 + 48c_3^4/35 + 108c_2^3c_4/7 + 3672c_3^2c_4^2/77 + 729c_4^4/13 + 264c_2^2c_3^2/35 + \\ 972c_2c_4^3/11 + 1296c_2c_3^2c_4/35 + 54c_2^2c_4^2 - 3$$

---

(2) Boundary Region for valid PM pdfs in the $|\gamma_3|$ and γ_4 plane:

---

(3) Lower (a) and Upper (b) Boundary Region points:

$$\bar\gamma_3 = 0, \bar\gamma_4 = -1.2^a; \quad \bar\gamma_3 = 0, \bar\gamma_4 = 0.7692^b; \quad \bar\gamma_3 = 1.529^b, \bar\gamma_4 = 1.312$$

---

(4) Conditions for valid PM pdfs in the Boundary Region:

$$0 < c_2 < 1; \quad c_4 > \frac{1}{9}(\sqrt{7}\sqrt{3 + 4c_2^2} - 7c_2)$$

Figure 2: The Conventional Power Method (PM) class of distributions based on the Uniform pdf in Figure 1.
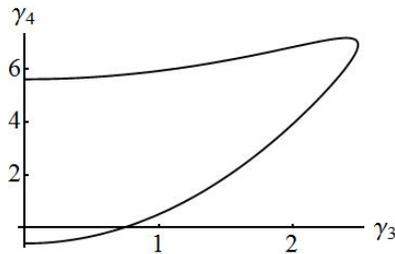
(1) Conventional Moment PM Triangular System:

$$\gamma_1 = 0 = c_1 + c_3$$

$$\gamma_2 = 1 = c_2^2 + 7c_3^2/5 + 24c_2c_4/5 + 54c_4^2/7$$

$$\gamma_3 = 21c_2^2c_3/5 + 88c_3^3/35 + 1116c_2c_3c_4/35 + 2214c_3c_4^2/35$$

$$\gamma_4 = 12c_2^4/5 + 327c_3^4/35 + 216c_2^3c_4/7 + 156924c_3^2c_4^2/385 + 46656c_4^4/91 + \\ 822c_2^2c_3^2/35 + 5184c_2c_4^3/11 + 6624c_2c_3^2c_4/35 + 864c_2^2c_4^2 - 3$$

---

(2) Boundary Region for valid PM pdfs in the $|\gamma_3|$ and γ_4 plane:

---

(3) Lower (a) and Upper (b) Boundary Region points:

$$\bar\gamma_3 = 0, \bar\gamma_4 = -0.60^a; \quad \bar\gamma_3 = 0, \bar\gamma_4 = 5.615^b; \quad \bar\gamma_3 = 2.484^b, \bar\gamma_4 = 6.924$$

---

(4) Conditions for valid PM pdfs in the Boundary Region:

$$0 < c_2 < 1; \quad c4 > \frac{1}{36}(\sqrt{21}\sqrt{8 + 13c2^2} - 21c_2)$$

Figure 3: The Conventional Power Method (PM) class of distributions based on the Triangular pdf in Figure 1.
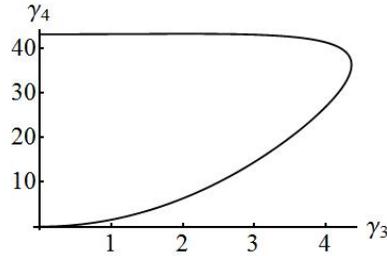
(1) Conventional Moment PM Normal System:

$$\gamma_1 = 0 = c_1 + c_3$$

$$\gamma_2 = 1 = c_2^2 + 2c_3^2 + 6c_2c_4 + 15c_4^2$$

$$\gamma_3 = 8c_3^3 + 6c_2^2c_3 + 72c_2c_3c_4 + 270c_3c_4^2$$

$$\gamma_4 = 3c_2^4 + 60c_2^2c_3^2 + 60c_3^4 + 60c_2^3c_4 + 936c_2c_3^2c_4 + 630c_2^2c_4^2 + 4500c_3^2c_4^2 + \\ 3780c_2c_4^3 + 10395c_4^4 - 3$$

---

(2) Boundary Region for valid PM pdfs in the $|\gamma_3|$ and γ_4 plane:

---

(3) Lower (a) and Upper (b) Boundary Region points:

$$\bar{\gamma}_3 = 0, \bar{\gamma}_4 = 0^a; \quad \bar{\gamma}_3 = 0, \bar{\gamma}_4 = 43.2^b; \quad \bar{\gamma}_3 = 4.363^b, \bar{\gamma}_4 = 36.34$$

---

(4) Conditions for valid PM pdfs in the Boundary Region:

$$0 < c_2 < 1; \quad c_4 > \frac{\sqrt{5 + 7c_2^2}}{5\sqrt{3}} - \frac{2c_2}{5}$$

Figure 4: The Conventional Power Method (PM) class of distributions based on the Normal pdf in Figure 1.
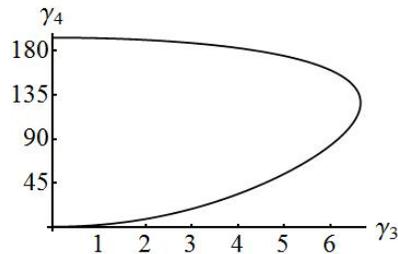
(1) Conventional Moment PM D-Logistic System:

$$\gamma_1 = 0 = c_1 + c_3$$

$$\gamma_2 = 1 = c_2^2 + 13c_3^2/5 + 36c_2c_4/5 + 180c_4^2/7$$

$$\gamma_3 = 39c_2^2c_3/5 + 592c_3^3/35 + 4644c_2c_3c_4/35 + 29052c_3c_4^2/35$$

$$\gamma_4 = 18c_2^4/5 + 1527c_3^4/7 + 720c_2^3c_4/7 + 10909512c_3^2c_4^2/385 + 59105376c_4^4/455$$
$$+6c_2^2(68c_3^2/35 + 1512c_4^2/5) + 4c_2c_4(5346c_3^2/7 + 58320c_4^2/11) - 3$$

---

(2) Boundary Region for valid PM pdfs in the $|\gamma_3|$ and γ_4 plane:

---

(3) Lower (a) and Upper (b) Boundary Region points:

$$\bar{\gamma}_3 = 0, \bar{\gamma}_4 = 0.60^a; \quad \bar{\gamma}_3 = 0, \bar{\gamma}_4 = 193.5^b; \quad \bar{\gamma}_3 = 6.652^b, \bar{\gamma}_4 = 127.0$$

---

(4) Conditions for valid PM pdfs in the Boundary Region:

$$0 < c_2 < 1; \quad c_4 > \frac{1}{120}(\sqrt{560 + 665c_2^2} - 35c_2)$$

Figure 5: The Conventional Power Method (PM) class of distributions based on the D-Logistic pdf in Figure 1.

(1) Conventional Moment PM Logistic System:

$$\gamma_1 = 0 = c_1 + c_3$$

$$\gamma_2 = 1 = c_2^2 + 16c_3^2/5 + 42c_2c_4/5 + 279c_4^2/7$$

$$\gamma_3 = 48c_2^2c_3/5 + 1024c_3^3/35 + 7488c_2c_3c_4/35 + 67824c_3c_4^2/35$$

$$\gamma_4 = 21c_2^4/5 + 6816c_2^2c_3^2/35 + 3840c_3^4/7 + 1116c_2^3c_4/7 + 51264c_2c_3^2c_4/7 + $$
$$20574c_2^2c_4^2/5 + 40384224c_3^2c_4^2/385 + 827820c_2c_4^3/11 + 343717911c_4^4/455 - 3$$

---

(2) Boundary Region for valid PM pdfs in the $|\gamma_3|$ and γ_4 plane:

---
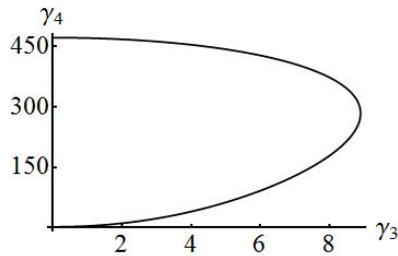
(3) Lower (a) and Upper (b) Boundary Region points:

$$\bar{\gamma}_3 = 0, \bar{\gamma}_4 = 1.2^a; \quad \bar{\gamma}_3 = 0, \bar{\gamma}_4 = 472.5^b; \quad \bar{\gamma}_3 = 8.913^b, \bar{\gamma}_4 = 283.9$$

---

(4) Conditions for valid PM pdfs in the Boundary Region:

$$0 < c_2 < 1; \quad c_4 > \frac{1}{93}(\sqrt{7}\sqrt{31 + 32c_2^2} - 21c_2)$$

Figure 6: The Conventional Power Method (PM) class of distributions based on the Logistic pdf in Figure 1.

coefficients, it is only necessary to consider positive values of γ_3 as simultaneous sign reversals between c_1 and c_3 will change the direction of γ_3 (i.e. from posistive to negative) but will have no effect on γ_2 or γ_4. For further details on other properties associated with PM distributions e.g. modes, median, trimmed means, etc., see [4] (pp. 9–15).

As indicated in the previous section, the polynomial transformation in (10) must be an increasing function in W for a PM distribution to have a valid pdf based on (11). Thus, it becomes necessary to determine the parameter space of γ_3 and γ_4 and the conditions that a set of solved coefficients must satisfy to yield a valid pdf for each of the five classes of PM distributions considered. This can be achieved by substituting the five sets of moments given in Table 1 into the following general expressions (see [4], p.18)

$$
\begin{aligned}
\bar{\gamma}_3 =& (2\mu_6^2)^{-1}(3(3/2)^{\frac{1}{2}}((c_2(3c_2 - \mu_4 5 c_2 + ((3c_2 - \mu_4 5 c_2)^2 - \mu_6 4(c_2^2 - 1))^{\frac{1}{2}})/\mu_6)^{\frac{1}{2}} \\
& (2\mu_6(\mu_8 - \mu_6) + c_2^2((9 - 13\mu_4)\mu_6^2 + \mu_6(5\mu_4 - 2\mu_8 - 3) + \mu_8(3 - 5\mu_4) - \\
& c_2((25\mu_4^2 - 4\mu_6 - 30\mu_4 + 9)c_2^2 + 4\mu_6)^{\frac{1}{2}}(\mu_8(5\mu_4 - 3) + \mu_6 - 3\mu_6^2)))
\end{aligned}
\tag{17}
$$

$$
\begin{aligned}
\bar{\gamma}_4 =& (1/(\mu_4 - 1)^2)(12\mu_4 - 3\mu_4^2 - 4\mu_6 + \mu_8 - 6 + c_2^4(3 + 10\mu_4^2 + \mu_4^3 + 2\mu_6 - \\
& \mu_4(6\mu_6 + 11) + \mu_8) + (1/\mu_6)(2c_2^3(3c_2 - 5c_2\mu_4 + ((3c_2 - 5c_2\mu_4)^2 - \\
& 4(c_2^2 - 1)\mu_6)^{\frac{1}{2}})(6\mu_4^3 - 5\mu_6 - 2\mu_4^2(\mu_6 + 3) + \mu_4(3 + 3\mu_6 - 2\mu_8) + 3\mu_8)) + \\
& (1/2\mu_6^2)(3c_2 - 5c_2\mu_4 + ((3c_2 - 5c_2\mu_4)^2 - 4(c_2^2 - 1)\mu_6)^{\frac{1}{2}})^2(3\mu_{10}(\mu_4 - 1) + \\
& 4\mu_6^2 + 6\mu_8 - \mu_6\mu_8 - 3\mu_4(\mu_6 + 2\mu_8))) + (1/16\mu_6^4)((3c_2 - 5c_2\mu_4 + \\
& ((3c_2 - 5c_2\mu_4)^2 - 4(c_2^2 - 1)\mu_6)^{\frac{1}{2}})^4(\mu_{12}(\mu_4 - 1)^2 + \mu_6(12(\mu_4 - 1)\mu_8 - \\
& 6\mu_{10}(\mu_4 - 1) - 4\mu_6^2 + \mu_6(\mu_8 + 3)))) - 2c_2^2(6\mu_4^2 - 3\mu_4 - \mu_6 - 3\mu_4\mu_6 + \mu_8 + \\
& (1/4\mu_6^2)((3c_2 - 5c_2\mu_4 + ((3c_2 - 5c_2\mu_4)^2 - 4(c_2^2 - 1)\mu_6)^{\frac{1}{2}})^2(3\mu_{10}(\mu_4 - 1) + \\
& 3\mu_4(10\mu_6 + \mu_6^2 - 4\mu_8) + (\mu_6 - 3)(\mu_6 - \mu_8) + \mu_4^2(7\mu_8 - 6 - 22\mu_6)))) - \\
& (1/\mu_6)(2c_2(3c_2 - 5c_2\mu_4 + ((3c_2 - 5c_2\mu_4)^2 - 4(c_2^2 - 1)\mu_6)^{\frac{1}{2}}) \times (3\mu_4^2 - 6\mu_6 + \\
& 2\mu_4(\mu_6 - \mu_8) + 3\mu_8 - (1/4\mu_6^2)((3c_2 - 5c_2\mu_4 + ((3c_2 - 5c_2\mu_4)^2 - \\
& 4(c_2^2 - 1)\mu_6)^{\frac{1}{2}})^2(\mu_{10}(1 + \mu_4 - 2\mu_4^2) + 6\mu_4^2\mu_8 + 3\mu_6(\mu_8 - 2\mu_6) + \\
& \mu_4(3\mu_6 + 2\mu_6^2 - 6\mu_8 - 2\mu_6\mu_8))))))
\end{aligned}
\tag{18}
$$

to determine the boundary regions of skew and kurtosis (denoted as $\bar{\gamma}_3$ and $\bar{\gamma}_4$), which are graphed in Figures 2–6. Further, the general conditions that the coefficients must satisfy to produce a valid PM pdf are given as in [4] (see p.17) are (a) $0 < c_2 < 1$ and (b)

$$
c_4 > \left(3c_2 - \mu_4 5 c_2 + ((3c_2 - \mu_4 5 c_2)^2 + \mu_6 4(1 - c_2^2))^{\frac{1}{2}}\right)/(2\mu_6)
\tag{19}
$$

where the specific conditions associated with (19) are also given in Figures 2–6 for each of the five classes of PM distributions.

In summary, Figure 2 through Figure 6 provide the systems of equations for solving polynomial coefficients, the boundary regions for valid PM pdfs, boundary points of maximum skew and minimum (maximum) kurtosis for symmetric distributions, and the conditions that solved coefficients must satisfy to produce a valid PM pdf. We subsequently give a brief introduction to L-moments and then provide the analogous details for the L-moment based third-order PM family of distributions as given in Figures 2–6 for the conventional family.

2.3 The *L*-moment third-order power method family

L-moments are defined as linear combinations of probability weighted moments β_i. In the context of the five classes of PM distributions considered herein, the β_i can be derived based on the general forms of (3), (4), and (10) as ([16])

$$\beta_i = \int p(w)\{F_W(w)\}^i f_W(w)\, dw \tag{20}$$

where $i = 0, \ldots, 3$. The first four L-moments are expressed as ([18, pp. 20-22])

$$\lambda_1 = \beta_0 \tag{21}$$
$$\lambda_2 = 2\beta_1 - \beta_0 \tag{22}$$
$$\lambda_3 = 6\beta_2 - 6\beta_1 + \beta_0 \tag{23}$$
$$\lambda_4 = 20\beta_3 - 30\beta_2 + 12\beta_1 - \beta_0. \tag{24}$$

The coefficients associated with β_i in (21)–(24) are determined from shifted orthogonal Legendre polynomials and are computed as shown in [10, p.20] or in [15].

The L-moments λ_1 and λ_2 in (21) and (22) are measures of location and scale and are the arithmetic mean and one-half of Gini's index of spread, respectively. Higher order L-moments are transformed to dimensionless quantities referred to as L-moment ratios defined as $\tau_r = \lambda_r/\lambda_2$ for $r \geq 3$, and where τ_3 and τ_4 are the analogs to the conventional measures of skew and kurtosis. In general, L-moment ratios are bounded in the interval $-1 < \tau_r < 1$ as is the index of L-skew (τ_3) where a symmetric distribution implies that all L-moment ratios with odd subscripts are zero. Other smaller boundaries can be found for more specific cases. For example, the index of L-kurtosis (τ_4) has the boundary condition for continuous distributions of (see [19])

$$\frac{5\tau_3^2 - 1}{4} < \tau_4 < 1. \tag{25}$$

In the context of the PM, integrating (20) using the pdf and cdf associated with (3) and (4) yields the β_i for each of the five classes of PM distributions

and subsequently substituting the β_i into (21)–(24) and simplifying yields the corresponding L-moment based systems of equations given in Figure 7 through Figure 11. Analogous to the conventional moment-based systems in Figure 2 through Figure 6, each of the five systems have four equations expressed in terms of four variables $c_1, \ldots, c_4$. The first two equations are standardized by setting $\lambda_1 = 0$ and λ_2 to its respective value of one-half of Gini's index given in Table 1. The last two equations are set to user specified values of τ_3 and τ_4. Similar to the conventional moment PM systems, if the negative of τ_3 is desired, then inspection of these five systems indicates that only simultaneous sign reversals are required between c_1 and c_3.

One of the advantages that the L-moment based PM systems have over the conventional PM systems is that they need not be numerically solved as the solutions to the coefficients are unique whenever they exist. Thus, closed-form expressions for the coefficients are also given in Figures 7–11.

The boundary conditions for valid third-order PM pdfs based on (11) can be generally determined by solving the quadratic equation $p'(w) = 0$ as

$$w = \frac{-c_3 \pm (c_3^2 - 3c_2c_4)^{\frac{1}{2}}}{3c_4}. \tag{26}$$

In general a set of solved coefficients with produce a valid pdf if the discriminant $c_3^2 - 3c_2c_4$ in (26) is negative. That is, the complex solutions for w must have non-zero imaginary parts. As such, setting $c_3^2 = 3c_2c_4$ will yield the point where the discriminant vanishes and thus real-valued solutions exist to $p'(w) = 0$.

There are more specific conditions associated with the coefficients that can be derived for evaluating if any given third-order PM distribution also has a valid pdf. For example, consider the uniform-based PM in Figure 7. If we set $\lambda_2 = 1/\sqrt{3}$ and subsequently solve for c_4 gives

$$c_4 = \frac{5}{9} - \frac{5c_2}{9}. \tag{27}$$

Substituting the right-hand side of (27) into the expressions for τ_3 and τ_4 in Figures 7 and setting $c_3 = (3c_2c_4)^{\frac{1}{2}}$, because we only need to consider positive values of L-skew, yields

$$\tau_3 = \frac{2\sqrt{c_2(1 - c_2)}}{\sqrt{5}} \tag{28}$$

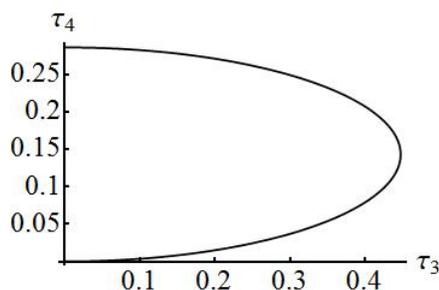$$\tau_4 = \frac{2}{7}(1 - c_2). \tag{29}$$

Inspection of (28) indicates that for real values of τ_3 to exist then we must have $c_2 \in [0, 1]$ and thus from (27) $c_4 \in [0, 5/9]$. Using (28) and (29), the graph of

(1) *L*-moment PM Uniform System:

$$\lambda_1 = 0 = c_1 + c_3 \qquad\qquad \lambda_2 = \frac{1}{\sqrt{3}} = \frac{5c_2 + 9c_4}{5\sqrt{3}}$$

$$\tau_3 = \frac{2\sqrt{3}c_3}{5c_2 + 9c_4} \qquad\qquad \tau_4 = \frac{18c_4}{35c_2 + 63c_4}$$

(2) Boundary Region for valid PM pdfs in the $|\tau_3|$ and τ_4 plane:

(3) Lower (a) and Upper (b) Boundary Region points:

$$\bar{\tau}_3 = 0, \bar{\tau}_4 = 0^a; \quad \bar{\tau}_3 = 0, \bar{\tau}_4 = 0.2857^b; \quad \bar{\tau}_3 = 0.4472^b, \bar{\tau}_4 = 0.1428$$

(4) Conditions for valid PM pdfs in the Boundary Region:

$$0 < c_2 < 1; \quad 0 < c_4 < \frac{5}{9}; \quad c_3^2 - 2c_2 c_4 < 0$$

(5) Closed-form solutions for coefficients:

$$c_1 = -c_3 \qquad\qquad c_2 = \frac{1}{2}(2 - 7\tau_4)$$

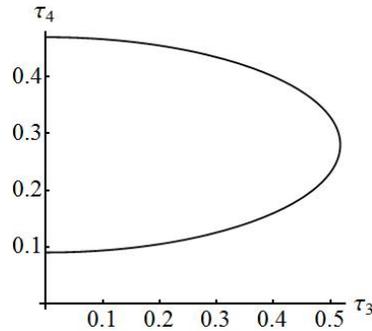$$c_3 = \frac{5\tau_3}{2\sqrt{3}} \qquad\qquad c_4 = \frac{35\tau_4}{18}$$

Figure 7: The *L*-moment Power Method (PM) class of distributions based on the Uniform pdf in Figure 1.

F. A. Hodis, T. C. Headrick, and Y. Sheng

(1) *L*-moment PM Triangular System:

$$\lambda_1 = 0 = c_1 + c_3 \qquad\qquad \lambda_2 = \frac{7}{5\sqrt{6}} = \frac{49c_2 + 108c_4}{35\sqrt{6}}$$

$$\tau_3 = \frac{71\sqrt{\frac{3}{2}}c_3}{98c_2 + 216c_4} \qquad\qquad \tau_4 = \frac{583c_2 + 6696c_4}{6468c_2 + 14256c_4}$$

---

(2) Boundary Region for valid PM pdfs in the $|\tau_3|$ and τ_4 plane:

---

(3) Lower (a) and Upper (b) Boundary Region points:

$$\bar\tau_3 = 0, \bar\tau_4 = 0.0901^a; \quad \bar\tau_3 = 0, \bar\tau_4 = 0.4697^b; \quad \bar\tau_3 = 0.5176^b, \bar\tau_4 = 0.2799$$

---

(4) Conditions for valid PM pdfs in the Boundary Region:

$$0 < c_2 < 1; \quad 0 < c_4 < \frac{49}{108}$$

---

(5) Closed-form solutions for coefficients:

$$c_1 = -c_3 \qquad\qquad c_2 = \frac{98(31 - 66\tau_4)}{2455}$$

$$c_3 = \tau_3 \frac{98}{71}\sqrt{\frac{2}{3}} \qquad\qquad c_4 = \frac{26411\tau_4}{22095} - \frac{28567}{265140}$$
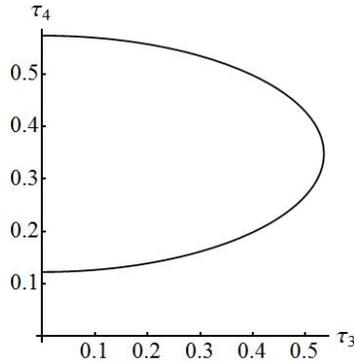
Figure 8: The *L*-moment Power Method (PM) class of distributions based on the Triangular pdf in Figure 1.

(1) *L*-moment PM Normal System:

$$\lambda_1 = 0 = c_1 + c_3 \qquad\qquad \lambda_2 = \frac{1}{\sqrt{\pi}} = \frac{4c_2 + 10c_4}{4\sqrt{\pi}}$$

$$\tau_3 = \frac{2c_3\sqrt{\frac{3}{\pi}}}{2c_2 + 5c_4} \qquad\qquad \tau_4 = \frac{20\sqrt{2}(c_2\delta_1 + c_4\delta_2)}{(2c_2 + 5c_4)\pi} - \frac{3}{2}$$

(2) Boundary Region for valid PM pdfs in the $|\tau_3|$ and τ_4 plane:

(3) Lower (a) and Upper (b) Boundary Region points:

$$\bar{\tau}_3 = 0, \bar{\tau}_4 = 0.1226^a; \quad \bar{\tau}_3 = 0, \bar{\tau}_4 = 0.5728^b; \quad \bar{\tau}_3 = 0.5352^b, \bar{\tau}_4 = 0.3472$$

(4) Conditions for valid PM pdfs in the Boundary Region:

$$0 < c_2 < 1; \quad 0 < c_4 < \frac{2}{5}; \quad c_3^2 - 2c_2c_4 < 0$$

(5) Closed-form solutions for coefficients:

$$c_1 = -c_3; \quad c_2 = \frac{-16\delta_2 + \sqrt{2}(3 + 2\tau_4)\pi}{8(5\delta_1 - 2\delta_2)}; \quad c_3 = \tau_3\sqrt{\frac{\pi}{3}}; \quad c_4 = \frac{40\delta_1 - \sqrt{2}(3 + 2\tau_4)\pi}{20(5\delta_1 - 2\delta_2)}$$
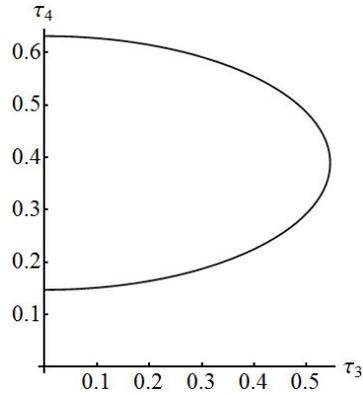
$$\delta_1 = \frac{3\tan^{-1}\sqrt{2}}{\sqrt{2}} - \frac{3\pi}{4\sqrt{2}}; \quad \delta_2 = \frac{15\tan^{-1}\sqrt{2}}{2\sqrt{2}} - \frac{15\pi}{8\sqrt{2}} + \frac{1}{4}$$

Figure 9: The *L*-moment Power Method (PM) class of distributions based on the Normal pdf in Figure 1.

(1) *L*-moment PM D-Logistic System:

$$\lambda_1 = 0 = c_1 + c_3 \qquad\qquad \lambda_2 = \frac{3+\pi^2}{3\sqrt{6}\pi} = \frac{18c_4\pi^2 + 5c_2(3+\pi^2)}{15\sqrt{6}\pi}$$

$$\tau_3 = \frac{\sqrt{\tfrac{3}{2}}c_3(45 - 75\pi^2 + 16\pi^4)}{90c_4\pi^3 + 25c_2\pi(3+\pi^2)} \qquad \tau_4 = \frac{21c_2\pi^4(-35+4\pi^2) + 15c_4(63 - 637\pi^4 + 72\pi^6)}{98\pi^2(18c_4\pi^2 + 5c_2(3+\pi^2))}$$

---

(2) Boundary Region for valid PM pdfs in the $|\tau_3|$ and τ_4 plane:

---

(3) Lower (a) and Upper (b) Boundary Region points:

$$\bar\tau_3 = 0, \bar\tau_4 = 0.1472^a; \quad \bar\tau_3 = 0, \bar\tau_4 = 0.6314^b; \quad \bar\tau_3 = 0.5452^b, \bar\tau_4 = 0.3893$$

---

(4) Conditions for valid PM pdfs in the Boundary Region:

$$0 < c_2 < 1; \qquad 0 < c_4 < \frac{5}{18} + \frac{5}{6\pi^2}; \qquad c_3^2 - 2c_2c_4 < 0$$

---

(5) Closed-form solutions for coefficients:

$$c_1 = -c_3 \qquad\qquad c_2 = \frac{5(3+\pi^2)(315 - 3185\pi^4 - 588\tau_4\pi^4 + 360\pi^6)}{4725 + 1575\pi^2 - 47775\pi^4 - 6115\pi^6 + 1296\pi^8}$$

$$c_3 = \frac{25\sqrt{\tfrac{2}{3}}\pi(3+\pi^2)\tau_3}{45 - 75\pi^2 + 16\pi^4} \qquad c_4 = -\frac{35\pi^2(3+\pi^2)(-210\tau_4 - 105\pi^2 - 70\tau_4\pi^2 + 12\pi^4)}{3(4725 + 1575\pi^2 - 47775\pi^4 - 6115\pi^6 + 1296\pi^8))}$$
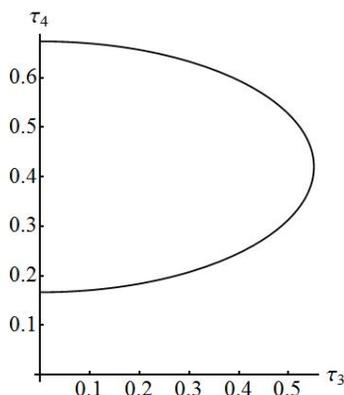
Figure 10: The *L*-moment Power Method (PM) class of distributions based on the D-Logistic pdf in Figure 1.

(1) *L*-moment PM Logistic System:

$$\lambda_1 = 0 = c_1 + c_3 \qquad \lambda_2 = \frac{\sqrt{3}}{\pi} = \frac{\sqrt{3}(c_2 + 3c_4)}{\pi}$$

$$\tau_3 = \frac{2\sqrt{3}c_3}{(c_2 + 3c_4)\pi} \qquad \tau_4 = \frac{c_2\pi^2 + 3c_4(30 + \pi^2)}{6(c_2 + 3c_4)\pi^2}$$

---

(2) Boundary Region for valid PM pdfs in the $|\tau_3|$ and τ_4 plane:

---

(3) Lower (a) and Upper (b) Boundary Region points:

$$\bar\tau_3 = 0, \bar\tau_4 = 0.1667^a; \quad \bar\tau_3 = 0, \bar\tau_4 = 0.6733^b; \quad \bar\tau_3 = 0.5513^b, \bar\tau_4 = 0.4200$$

---

(4) Conditions for valid PM pdfs in the Boundary Region:

$$0 < c_2 < 1; \quad 0 < c_4 < \frac{1}{3}; \quad c_3^2 - 2c_2c_4 < 0$$

---

(5) Closed-form solutions for coefficients:

$$c_1 = -c_3 \qquad c_2 = \frac{1}{30}(30 + \pi^2 - 6\pi^2\tau_4)$$

$$c_3 = \frac{\tau_3\pi}{2\sqrt{3}} \qquad c_4 = \frac{1}{90}(6\pi^2\tau_4 - \pi^2)$$

Figure 11: The *L*-moment Power Method (PM) class of distributions based on the Logistic pdf in Figure 1.

the region for valid pdfs is given in Figure 7 along with minimum and maximum values of τ_3 and τ_4. The derivations of the other four PM boundary regions and boundary points are analogous to the uniform-based PM transformation. The boundary regions, boundary points, and specific conditions for coefficients to ensure a valid PM pdf for the other four classes of distributions are given in Figures 8–11.

Figure 12 through Figure 16 provide examples of the graphs of PM pdfs based on selected values of τ_3 and τ_4 from each of five classes of distributions. The solved coefficients for each PM distribution are provided as well as their corresponding values of conventional skew (γ_3), kurtosis (γ_4), and coefficients. These distributions are subsequently used in the simulation portion of the study, which is presented in the next section.

3 A comparison between the Conventional moment and *L*-moment families

3.1 Estimation

One of the advantages that sample *L*-moment ratios ($t_{3,4}$) have over conventional moment based estimators, such as skew (g_3) and kurtosis (g_4), is that $t_{3,4}$ are less biased (e.g. [18]). This advantage can be demonstrated in the context of the PM by considering the simulation results associated with the indices for the percentage of relative bias and standard error reported in Figure 12 through Figure 16. More specifically, a Fortran algorithm was coded to generate twenty-five thousand independent sample estimates of $g_{3,4}$ and $t_{3,4}$ based on the parameters and coefficients listed in Figures 12–16. The estimates of $g_{3,4}$ were computed based on Fisher?s k-statistics and the estimates of $t_{3,4}$ were based on the formulae given in Headrick ([4], Eqs. 6, 8). Both small ($n = 50$) and large ($n = 1000$) sample sizes were considered. Bootstrapped average estimates, confidence intervals, and standard errors were obtained for $g_{3,4}$ and $t_{3,4}$ using ten-thousand resamples via the commercial software package Spotfire S+ [20]. Further, the percentage of relative bias (RBias) for each estimate was computed as: RBias %(g_j)= $100 \times (g_j - \gamma_j)/\gamma_j$ and RBias %(t_j)= $100 \times (t_j - \tau_j)/\tau_j$.

The results in Figures 12–16 demonstrate the substantial advantage that *L*-moment ratios have over conventional moment estimates in terms of both relative bias and error and for all classes of PM distributions considered. For example, in the context of the logistic based PM ($n = 1000$), the conventional estimates of g_3 and g_4 generated in the simulation were, on average, 30% and 67% less than their respective parameters. On the other hand, the amounts of relative bias associated with the *L*-moment ratios are essentially negligible.
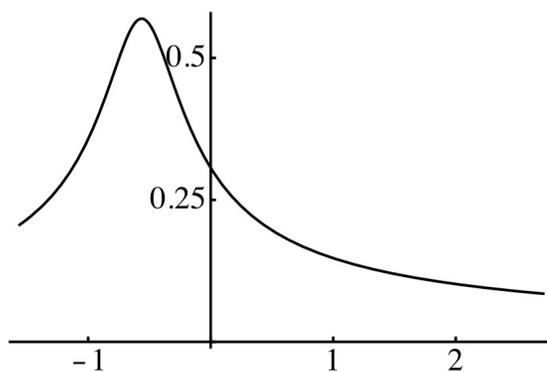
L-moment

Parameters and Coefficients:

$\tau_3 = 0.20$
$\tau_4 = 0.10$
$\qquad c_1 = -0.2887, c_2 = 0.6500, c_3 = 0.2887, c_4 = 0.1944$

Estimate	95% Bootstrap C.I.	Standard Error	Relative Bias %
$t_3 = 0.2012$	$0.2005, 0.2018$	0.0003	0.60
$t_4 = 0.1038$	$0.1032, 0.1044$	0.0003	3.80

Conventional Moment

Parameters and Coefficients:

$\gamma_3 = 0.811$
$\gamma_4 = -0.201$
$\qquad c_1 = -0.2765, c_2 = 0.6226, c_3 = 0.2765, c_4 = 0.1862$

Estimate	95% Bootstrap C.I.	Standard Error	Relative Bias %
$g_3 = 0.8231$	$0.8201, 0.8261$	0.0015	1.54
$g_4 = -0.0397$	$-0.0488, -0.0315$	0.0044	80.2

Figure 12: Simulation results of an example that compares the Conventional and *L*-moment Uniform PM classes. The estimates were based on sample sizes of $n = 50$.
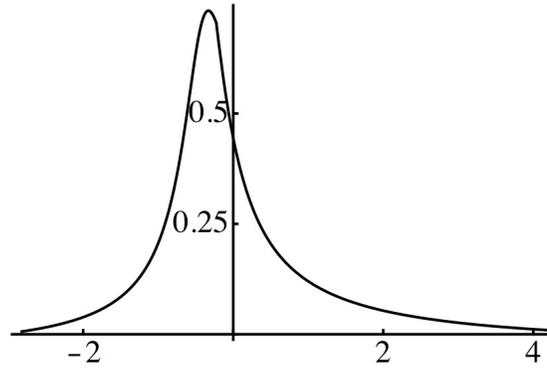
$$L\text{-moment}$$

Parameters and Coefficients:

$\tau_3 = 0.20$
$\tau_4 = 0.25$
  $c_1 = -0.2254, c_2 = 0.5788, c_3 = 0.2254, c_4 = 0.1911$

Estimate	95% Bootstrap C.I.	Standard Error	Relative Bias %
$t_3 = 0.1970$	$0.1959, 0.1980$	0.0005	-1.50
$t_4 = 0.2515$	$0.2508, 0.2522$	0.0004	0.60

Conventional Moment

Parameters and Coefficients:

$\gamma_3 = 1.235$
$\gamma_4 = 2.627$
  $c_1 = -0.2042, c_2 = 0.5243, c_3 = 0.2042, c_4 = 0.1731$

Estimate	95% Bootstrap C.I.	Standard Error	Relative Bias %
$g_3 = 1.140$	$1.134, 1.147$	0.0032	-7.69
$g_4 = 2.492$	$2.467, 2.514$	0.0120	-5.10

Figure 13: Simulation results of an example that compares the Conventional and L-moment Triangular PM classes. The estimates were based on sample sizes of $n = 50$.
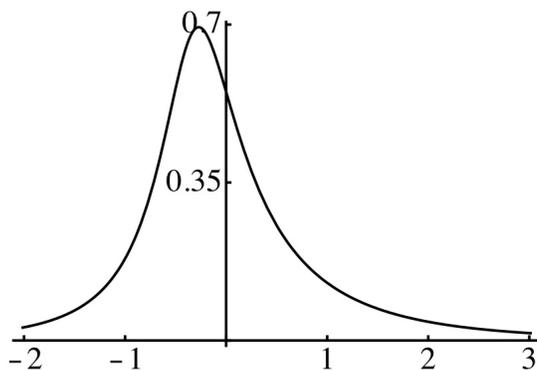
L-moment

Parameters and Coefficients:

$\tau_3 = 0.15$
$\tau_4 = 0.30$
$\qquad c_1 = -0.1535, c_2 = 0.6059, c_3 = 0.1535, c_4 = 0.1576$

Estimate	95% Bootstrap C.I.	Standard Error	Relative Bias %
$t_3 = 0.1426$	$0.1410, 0.1442$	0.0008	-4.93
$t_4 = 0.2948$	$0.2939, 0.2958$	0.0005	-1.73

Conventional Moment

Parameters and Coefficients:

$\gamma_3 = 1.546$
$\gamma_4 = 12.64$
$\qquad c_1 = -0.1316, c_2 = 0.5196, c_3 = 0.1316, c_4 = 0.1352$

Estimate	95% Bootstrap C.I.	Standard Error	Relative Bias %
$g_3 = 0.9860$	$0.9695, 1.002$	0.0082	-36.2
$g_4 = 5.365$	$5.302, 5.432$	0.0327	-57.6

Figure 14: Simulation results of an example that compares the Conventional and L-moment Normal PM classes. The estimates were based on sample sizes of $n = 50$.
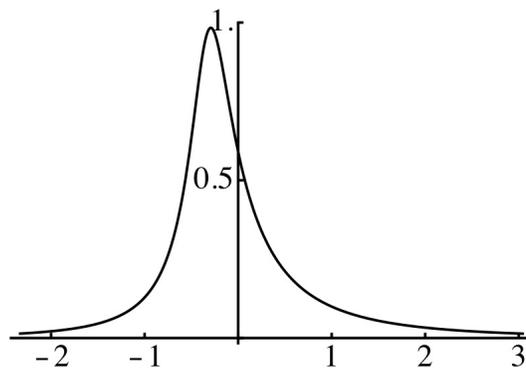
L-moment

Parameters and Coefficients:

$\tau_3 = 0.20$
$\tau_4 = 0.40$

$c_1 = -0.1912, c_2 = 0.4779, c_3 = 0.1912, c_4 = 0.1891$

Estimate	95% Bootstrap C.I.	Standard Error	Relative Bias %
$t_3 = 0.1993$	$0.1987, 0.1999$	0.0003	-0.35
$t_4 = 0.3991$	$0.3988, 0.3994$	0.0002	-0.22

Conventional Moment

Parameters and Coefficients:

$\gamma_3 = 3.234$
$\gamma_4 = 80.70$

$c_1 = -0.1389, c_2 = 0.3473, c_3 = 0.1389, c_4 = 0.1374$

Estimate	95% Bootstrap C.I.	Standard Error	Relative Bias %
$g_3 = 2.621$	$2.587, 2.654$	0.0172	-5.50
$g_4 = 43.10$	$42.53, 43.67$	0.2948	-46.6

Figure 15: Simulation results of an example that compares the Conventional and *L*-moment D-Logistic PM classes. The estimates were based on sample sizes of $n = 1000$.
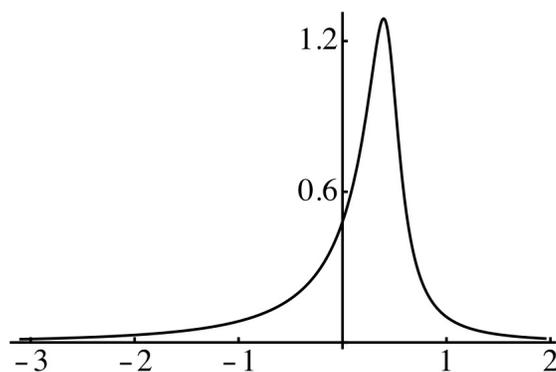
L-moment

Parameters and Coefficients:

$\tau_3 = -0.30$
$\tau_4 = 0.45$

$c_1 = 0.2721, c_2 = 0.4407, c_3 = -0.2721, c_4 = 0.1864$

Estimate	95% Bootstrap C.I.	Standard Error	Relative Bias %
$t_3 = -0.2989$	$-0.2997, -0.2983$	.0004	-0.37
$t_4 = 0.4484$	$0.4480, 0.4488$	.0002	-0.36

Conventional Moment

Parameters and Coefficients:

$\gamma_3 = -6.099$
$\gamma_4 = 232.3$

$c_1 = -0.1718, c_2 = 0.2784, c_3 = 0.1718, c_4 = 0.1178$

Estimate	95% Bootstrap C.I.	Standard Error	Relative Bias %
$g_3 = -4.269$	$-4.318, -4.217$	0.0257	-30.0
$g_4 = 76.58$	$75.57, 77.62$	0.5151	-67.0

Figure 16: Simulation results of an example that compares the Conventional and L-moment Logistic PM classes. The estimates were based on sample sizes of $n = 1000$.

Further, the standard errors associated with $t_{3,4}$ are relatively much smaller than the corresponding standard errors for $g_{3,4}$.

3.2 Power

Hosking [21] suggested that L-skew (τ_3) and L-kurtosis (τ_4) are more accurate indicators of the power associated with goodness-of-fit tests in terms of detecting deviations from normality than the usual measures of skew (γ_3) and kurtosis (γ_4). This advantage can also be demonstrated in the context of PM transformations. Specifically, listed in Table 2 are values of γ_4 and τ_4 for the normal distribution and twenty-one other various symmetric non-normal distributions based on the Normal, D-logistic, and Logistic PM transformations. To make the comparison, an algorithm was coded in Fortran to draw twenty-five thousand independent samples of size $n = 20$ from each of the twenty-two

Case	PM Polynomial	Kurtosis (γ_4)	L-kurtosis (τ_4)	Power
1	Normal	0	0.1226	0.05
2	Normal	1	0.1586	0.094
3	Logistic	2	0.1779	0.131
4	D-Logistic	3	0.1858	0.155
5	Normal	4	0.2195	0.229
6	D-Logistic	5	0.2040	0.201
7	Logistic	6	0.2073	0.203
8	Logistic	7	0.2120	0.215
9	Normal	8	0.2715	0.378
10	Normal	9	0.2824	0.411
11	Logistic	10	0.2238	0.246
12	D-Logistic	12	0.2438	0.302
13	D-Logistic	14	0.2522	0.323
14	Normal	16	0.3485	0.604
15	Normal	18	0.3656	0.651
16	D-Logistic	20	0.2739	0.378
17	Logistic	25	0.2604	0.336
18	Normal	30	0.4623	0.866
19	D-Logistic	35	0.3160	0.487
20	Normal	40	0.5447	0.968
21	D-Logistic	45	0.3394	0.545
22	Logistic	50	0.2978	0.431

Table 2: Power of the Anderson-Darling test for normality ($\alpha = 0.05$) for various symmetric power method (PM) distributions. Each entry of power is based on a sample size of $n = 20$. See Figure 17.
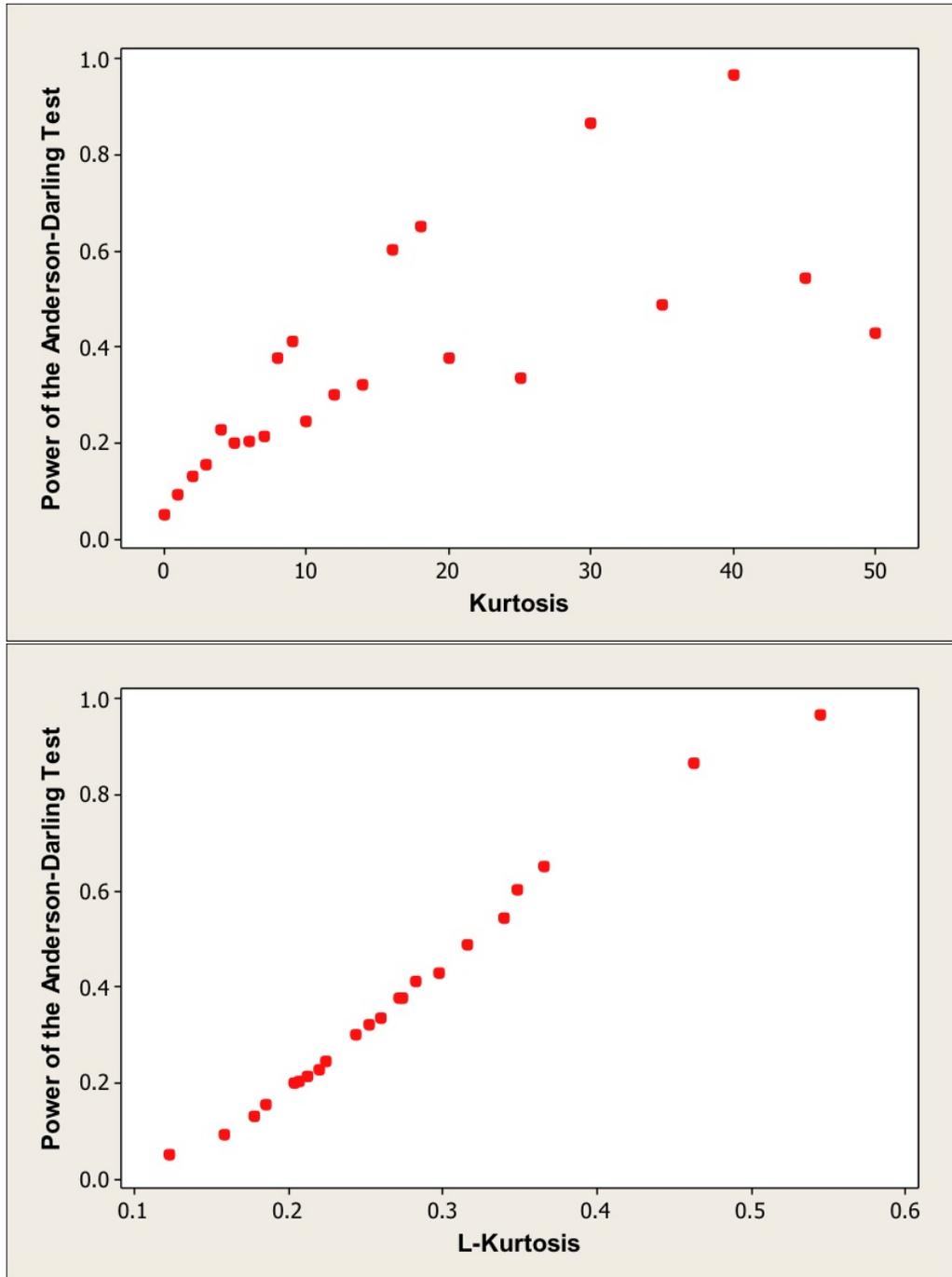
Figure 17: Power of the Anderson-Darling test for the kurtosis and *L*-kurtosis values associated with the symmetric power method distributions in Table 2.

distributions. The Anderson-Darling (AD) test [22] was computed to test for normality ($\alpha = 0.05$) on each sample. The power results associated with the AD test are given in Table 2 and represent the proportion of rejections across the twenty-five thousand replications.

Figure 17 gives the plots of the power of the AD test against kurtosis (γ_4) and L-kurtosis (τ_4). Inspection of Figure 17 indicates that, with the exception of small departures from normality, the relationship between γ_4 and power to be erratic whereas the relationship between τ_4 and power is very well defined. Thus, τ_4 is the more appropriate index for distinguishing between distributions as it relates to the power of the AD test. Similar results were also reported in [21] in the context of the Shapiro-Wilk test for normality.

3.3   Outliers

Another advantage that L-moments have over conventional moments is that they are relatively insensitive to extreme scores or outliers (e.g. [17]). This can be demonstrated by considering the two skewed and heavy-tailed standard normal PM distributions given in Table 3. Specifically, five samples of size $n = 5000$ were drawn from each of these two distributions and the estimates of skew (L-skew) and kurtosis (L-kurtosis) were computed on all the data points and again after the single largest data point was removed from each of the data sets. The estimates are listed in Table 3 where an entry enclosed in parentheses represents an estimate for a data set after the largest data point had been removed. Presented in Panel A (Panel B) of Figure 18 is a plot that summarizes the ten data sets in the skew (L-skew) and kurtosis (L-kurtosis) plane. A circle in the plane represents a data set with all values included and a square represents a data set with its largest value removed.

Given a sample size of $n = 5000$, one might expect that both conventional moments and L-moments would be relatively insensitive to the removal of a single data point. However, inspection of Figure 18 indicates that there is no discernable pattern that would allow one to predict what the effect might be on the conventional measures of skew or kurtosis. For example, removing the largest data point from the second sample associated with the first population had the effect of reducing skew by 9.94% and reducing kurtosis by 13.92%. On the other hand, removing the largest data point from the first sample associated with the second population had the effect of reducing skew by 41.35% and reducing kurtosis by 43.63%. More generally, the effect of deleting the single largest value from a data set can produce large, moderate, or small changes in skew and kurtosis.

In terms of L-skew and L-kurtosis, inspection of Figure 18 indicates that there is a clear predictive pattern of what the effects are from removing the largest data point – a consistent slight shift down and to the left in the plane

Parameters	Sample	Skew g_3	Kurtosis g_4	*L*-skew t_3	*L*-kurtosis t_4
Population A	1	1.849	18.334	.1635	.3600
$\gamma_3 = 2.0$		(1.428)	(12.552)	(.1591)	(.3570)
$\gamma_4 = 20$					
	2	1.991	15.616	.1738	.3673
$\tau_3 = .182804$		(1.793)	(13.443)	(.1704)	(.3651)
$\tau_4 = .359955$					
	3	2.006	15.936	.1878	.3530
		(1.671)	(11.414)	(.1838)	(.3503)
	4	1.854	20.929	.1852	.3590
		(1.362)	(13.986)	(.1807)	(.3558)
	5	1.999	25.008	.1744	.3630
		(1.281)	(13.434)	(.1691)	(.3593)
Population B	1	2.808	48.603	.3118	.4997
$\gamma_3 = 3.5$		(1.647)	(27.398)	(.3054)	(.4956)
$\gamma_4 = 40$					
	2	3.684	33.757	.3517	.4808
$\tau_3 = .330319$		(3.194)	(25.328)	(.3472)	(.4778)
$\tau_4 = .499842$					
	3	3.095	37.977	.3234	.5090
		(2.604)	(30.879)	(.3186)	(.5061)
	4	3.509	41.026	.3309	.4988
		(3.095)	(35.237)	(.3262)	(.4979)
	5	4.014	39.106	.3648	.5013
		(3.355)	(26.425)	(.3597)	(.4979)

Table 3: Sample statistics from two populations (A and B) based on samples of size $n = 5000$. The samples were drawn from normal-based PM polynomials. An entry enclosed in parentheses denotes a statistic that was computed on the data set after the single largest value had been removed (i.e. $n = 4999$). See Figure 18.
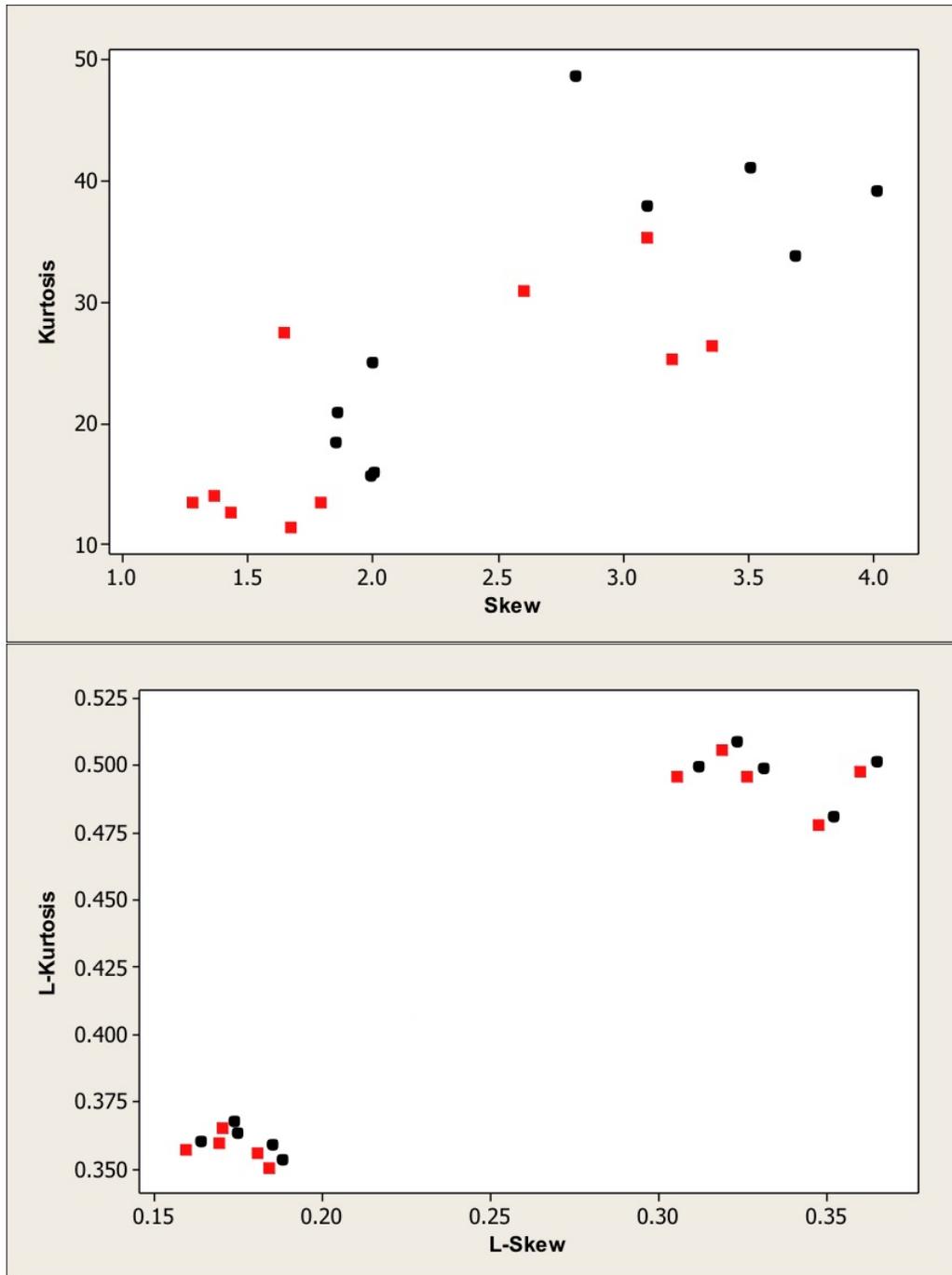
F. A. Hodis, T. C. Headrick, and Y. Sheng

Figure 18: Plots of the Skew-Kurtosis and *L*-skew-*L*-kurtosis values listed in Table 3. Black circles denote statistics based on samples of size $n = 5000$ and red squares denote statistics based on the same samples with their largest value deleted ($n = 4999$).
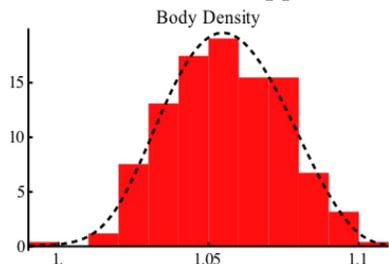
– i.e. slightly less *L*-skew and slightly less *L*-kurtosis. One way of making a comparison on a percentage basis to what was done above is to convert the values of *L*-skew and *L*-kurtosis in Table 3 to the conventional measures of skew and kurtosis. This is accomplished by evaluating the third-order system of equations in Figure 9 using the coefficients that would yield the values of *L*-skew and *L*-kurtosis in Table 3. For example, the values of $t_3 = .1738$ (.1704) and $t_4 = .3673$ (.3651) associated with the second sample in the first population would convert to the values of $g_3 = 1.925$ (1.887) and $g_4 = 20.615$ (20.274). Thus, removing the largest data point from the second sample of the first population would have the effect of reducing skew and kurtosis by only 1.97% and 1.65%, respectively. Similarly, removing the largest data point from the first sample associated with the second population would have the effect of reducing skew and kurtosis by only 1.64% and 1.53%.

3.4 Distribution Fitting

Presented in Figure 19 are conventional moment and *L*-moment-based PM pdfs superimposed on a histogram of body density data taken from adult males (http://lib.stat.cmu.edu/datasets/bodyfat). The data were measured in grams per cubic centimeter. The PM pdfs are based on fifth-order polynomials i.e. $m = 6$ in (5) as third-order polynomials yielded less accurate fits to the data. The conventional and *L*-moment based sample estimates of $g_{3,...,6}$ and $t_{3,...,6}$ listed in Figure 19 were based on a sample size of $n = 252$ participants. The conventional estimates of $g_{3,...,6}$ and their coefficients were computed using the Mathematica source code given in [23]. The *L*-moment ratios $t_{3,...,6}$ and their coefficients were computed using the formulae given in [16] (see Eqs. 6, 8; and Eqs. 10–15). The sample estimates were subsequently used to solve for the two sets of coefficients, which produced the PM pdfs based on (11). Note that the two polynomials were linearly transformed using the location and scale estimates $(m, s; \ell_1, \ell_2)$ from the data.

Visual inspection of the PM approximations in Figure 19 and the goodness of fit statistics given in Table 4 indicate that the *L*-moment-based pdf provides a more accurate fit to the actual data. The reason for this is partially attributed to the fact that the conventional moment-based power method pdf does not have an exact match with g_6 whereas the *L*-moment pdf is based on an exact match with all of the sample estimates. Note also that the asymptotic *p*-values in Table 4 are based on a chi-square distribution with degrees of freedom: $df = 10(\text{classes}) - 6(\text{estimates}) - 1(\text{sample size}) = 3$.

Conventional moment approximation　　　　　*L*-moment approximation
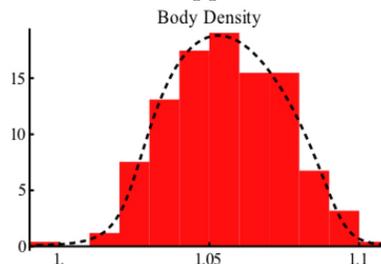
Parameter Estimates	Coefficients	Parameter Estimates	Coefficients
$m = 1.055574$	$c_1 = -0.006154$	$\ell_1 = 1.055574$	$c_1 = -0.013362$
$s = 0.019031$	$c_2 = 1.071691$	$\ell_2 = 0.010850$	$c_2 = 1.118827$
$g_3 = -0.020176$	$c_3 = 0.016487$	$t_3 = 0.003546$	$c_3 = 0.035260$
$g_4 = -0.309619$	$c_4 = -0.033401$	$t_4 = 0.086880$	$c_4 = -0.079607$
$g_5 = -0.400378$	$c_5 = -0.003444$	$t_5 = -0.009142$	$c_5 = -0.007300$
$g_6 = 2.368240$	$c_6 = 0.001831$	$t_6 = 0.038191$	$c_6 = 0.007460$

Figure 19: Histograms and fifth-order power method approximations for the Body Density Data taken from $n = 252$ adult males.

%	Expected	Obs(C)	Obs(L)	Body Density (C)	Body Density (L)
10	25.2	25	25	<1.03087	<1.03120
20	25.2	27	25	1.03087–1.03885	1.03120–1.03847
30	25.2	24	26	1.03885–1.04494	1.03847–1.04443
40	25.2	28	24	1.04494–1.05032	1.04443–1.04994
50	25.2	25	29	1.05032–1.05546	1.04994–1.05532
60	25.2	22	23	1.05546–1.06064	1.05532–1.06079
70	25.2	21	22	1.06064–1.06615	1.06079–1.06656
80	25.2	27	28	1.06615–1.07245	1.06656–1.07298
90	25.2	29	26	1.07245–1.08072	1.07298–1.08090
100	25.2	24	24	>1.08072	>1.08090

$$\text{C: } \chi^2 = 2.365 \qquad\qquad L\text{: } \chi^2 = 1.651$$
$$\Pr\{\chi_3^2 \le 2.365\} = .500 \qquad \Pr\{\chi_3^2 \le 1.651\} = .648$$

Table 4: Chi-square goodness of fit statistics for the conventional (C) moment and *L*-moment approximations for the Body Density Data ($n = 252$) depicted in Figure 19.

4 Concluding Comments

This paper presented five classes of PM distributions in the contexts of both conventional moments and L-moments. The inclusion of the four additional classes of PM distributions beyond the standard normal based PM substantially broadens the boundary of feasible combinations of skew (L-skew) and kurtosis (L-kurtosis). Specifically, in the context of symmetric third-order polynomials, the conventional kurtosis boundary was extended from $0 < \gamma_4 < 43.2$ to $-1.2 < \gamma_4 < 472.5$ where the lower limit is associated with the uniform distribution and the upper limit is associated with the logistic-based PM transformation.

The conventional moment and L-moment families of PM distributions were also compared in terms of estimation, power, outliers, distribution fitting. In all four categories, the L-moment based PM family was superior to the conventional moment family. Thus, the L-moment based PM is an attractive alternative to the traditional or conventional PM. In particular, the L-moment based procedure has distinct advantages when distributions with large departures from normality are under consideration. Finally, we would note that Mathematica 8.0.1 source code is available from the authors for implementing procedures associated with either the conventional or L-moment families of PM distributions e.g. solving for coefficients, computing percentage points, graphing pdfs, and so forth.

References

[1] A. I. Fleishman, A method for simulating non-normal distributions, *Psychometrika,* **43** (1978), 521–532.

[2] C. D. Vale and V. A. Maurelli, Simulating multivariate nonnormal distributions, *Psychometrika,* **48** (1983), 465–471.

[3] T. C. Headrick, Fast fifth-order polynomial transforms for generating univariate and multivariate non-normal distributions, *Computational Statistics and Data Analysis,* **40** (2002), 685–711.

[4] T. C. Headrick, *Statistical Simulation: Power Method Polynomials and Other Transformations,* Chapman & Hall/CRC, Boca Raton, FL, 2010.

[5] M. R. Harwell and R. C. Serlin, An empirical study of a proposed test of nonparametric analysis of covariance, *Psychological Bulletin,* **104** (1988), 268–281.

[6] T. C. Headrick and S. S. Sawilowsky, Properties of the rank transformation in factorial analysis of covariance, *Communications in Statistics: Simulation and Computation,* **29** (2000), 1059–1087.

[7] J. Affleck-Graves and B. MacDonald, Nonnormalities and tests of asset pricing theories, *Journal of Finance,* **44** (1989), 889–908.

[8] C. Stone, Empirical power and type I error rates for an IRT fit statistic that considers the precision and ability estimates, *Educational and Psychological Measurement,* **63** (2003), 566–583.

[9] D. A. Powell, L. M. Anderson, R. Y. S. Chen, and W. G. Alvord, Robustness of the Chen-Dougherty-Brittner procedure against non-normality and heterogeneity distribution in the coefficient of variation, *Journal of Biomedical Optics,* **7** (2002), 650–660.

[10] H. S. Steyn, On the problem of more than one kurtosis parameter in multivariate analysis, *Journal of Multivariate Analysis,* **44** (1993), 1–22.

[11] T. M. Beasley and B. D. Zumbo, Comparison of aligned Friedman rank and parametric methods for testing interactions in split-plot designs, *Computational Statistics and Data Analysis,* **42** (2003), 569–593.

[12] O. Mahul, Hedging price risk in the presence of crop yield and revenue insurance, *European Review of Agricultural Economics,* **30** (2003), 217–239.

[13] T. C. Headrick and O. Rotou, An investigation of the rank transformation in multiple regression, *Computational Statistics and Data Analysis,* **50** (2001), 3343–3353.

[14] J. M. Henson, S. P. Reise, and K. H. Kim, Detecting mixtures from structural model differences using latent variable mixture modeling: A comparison of relative model fit statistics, *Structural Equation Modeling,* **14** (2007), 202–226.

[15] L. Hothorn and W. Lehmacher, A simple testing procedure ?control versus k treatments? for one-sided ordered alternatives, with application in toxicology, *Biometrical Journal,* **33** (2007), 179–189.

[16] T. C. Headrick, A characterization of power method transformations through *L*-moments, *Journal of Probability and Statistics,* **vol. 2011**, Article ID 497463, 22 pages, 2011.

[17] J. R. M. Hosking, *L*-moments: Analysis and estimation of distributions using linear combinations of order statistics, *Journal of the Royal Statistical Society, Series B,* **52** (1990), 105–124.

[18] J. R. M. Hosking and J. R. Wallis, *Regional Frequency Analysis: An Approach Based on* L-*moments,* Cambridge University Press, Cambridge, UK., 1997.

[19] M. C. Jones, On some expressions for variance, covariance, skewness, and *L*-moments, *Journal of Statistical Planning and Inference,* **126** (2004), 97–106.

[20] TIBCO, *Spotfire S+ 8.1 for Windows,* TIBCO Software, Palo Alto, CA, 2008.

[21] J. R. M. Hosking, Moments or *L*-moments? An example comparing two measures of distributional shape, *American Statistician,* **46** (1992), 186–189.

[22] T. W. Anderson and D. A. Darling, D. A., Asymptotic theory of certain ?goodness-of-fit? criteria based on stochastic processes, *Annals of Mathematical Statistics,* **23** (1952), 193–212.

[23] T. C. Headrick, Y. Sheng, and F. A. Hodis, Numerical computing and graphics for the power method transformation using Mathematica, *Journal of Statistical Software,* **19** (2007), 1–17.